



The Abdus Salam
International Centre for Theoretical Physics

United Nations
Educational, Scientific
and Cultural Organization



SMR 1673/54

AUTUMN COLLEGE ON PLASMA PHYSICS

5 - 30 September 2005

Shear-driven fluctuations in magnetized plasma: theory and lab comparisons PART II

M. KOEPKE

Physics Dept., West Virginia University,
Morgantown, USA

Shear-driven fluctuations in magnetized plasma: Space and lab comparisons

Mark Koepke

Physics Dept., West Virginia University, Morgantown, WV 26506 USA

work supported by U.S. National Science Foundation

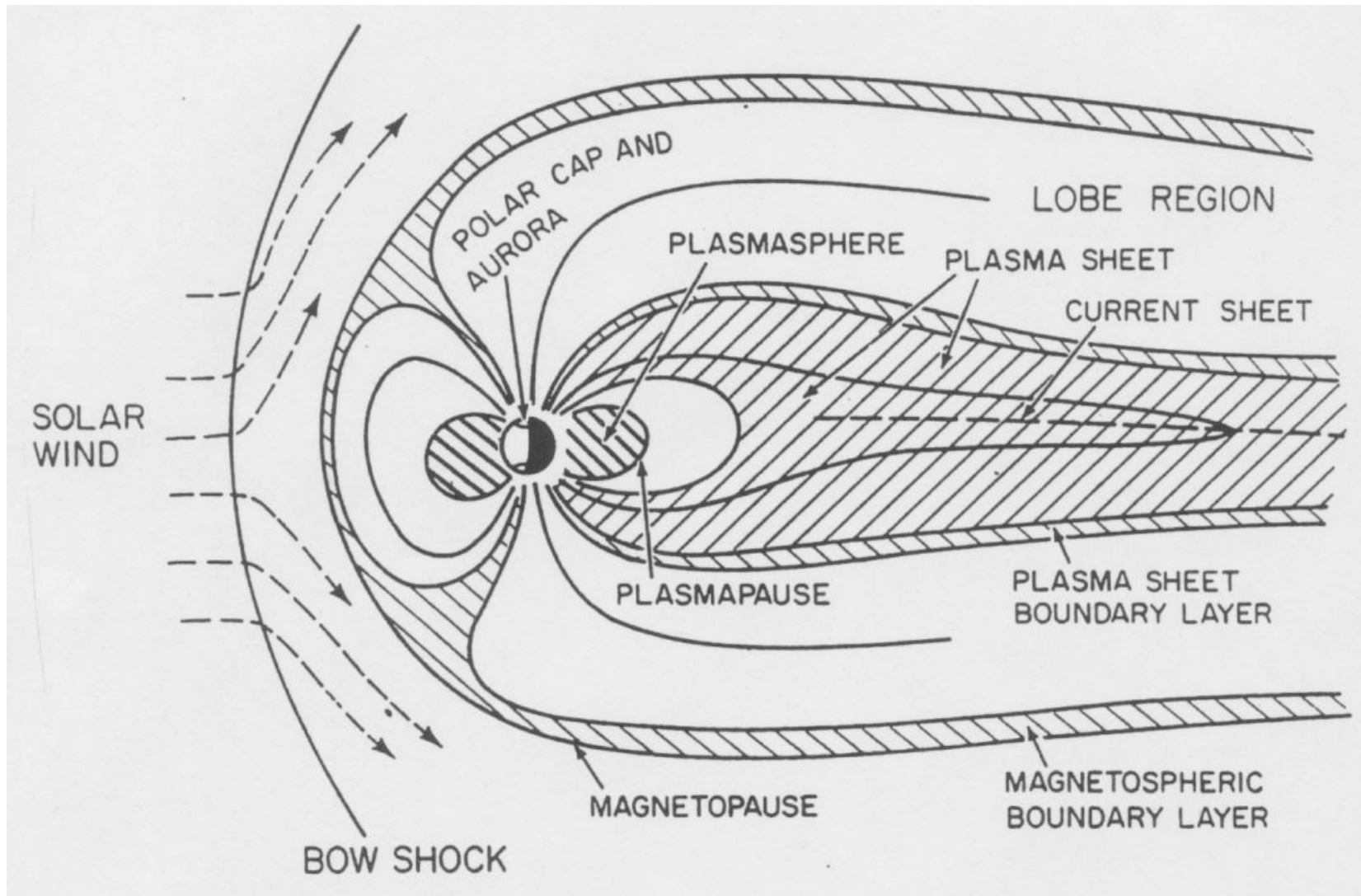
*Useful discussions with J. Bonnell, P. Kintner, M. Andre, D. Knudsen,
V. Gavriishchaka, G. Ganguli, C. Teodorescu, E. Reynolds,
R. Hatakeyama, T. Kaneko, E. Scime, & R. Merlino are gratefully acknowledged.*

Space observations

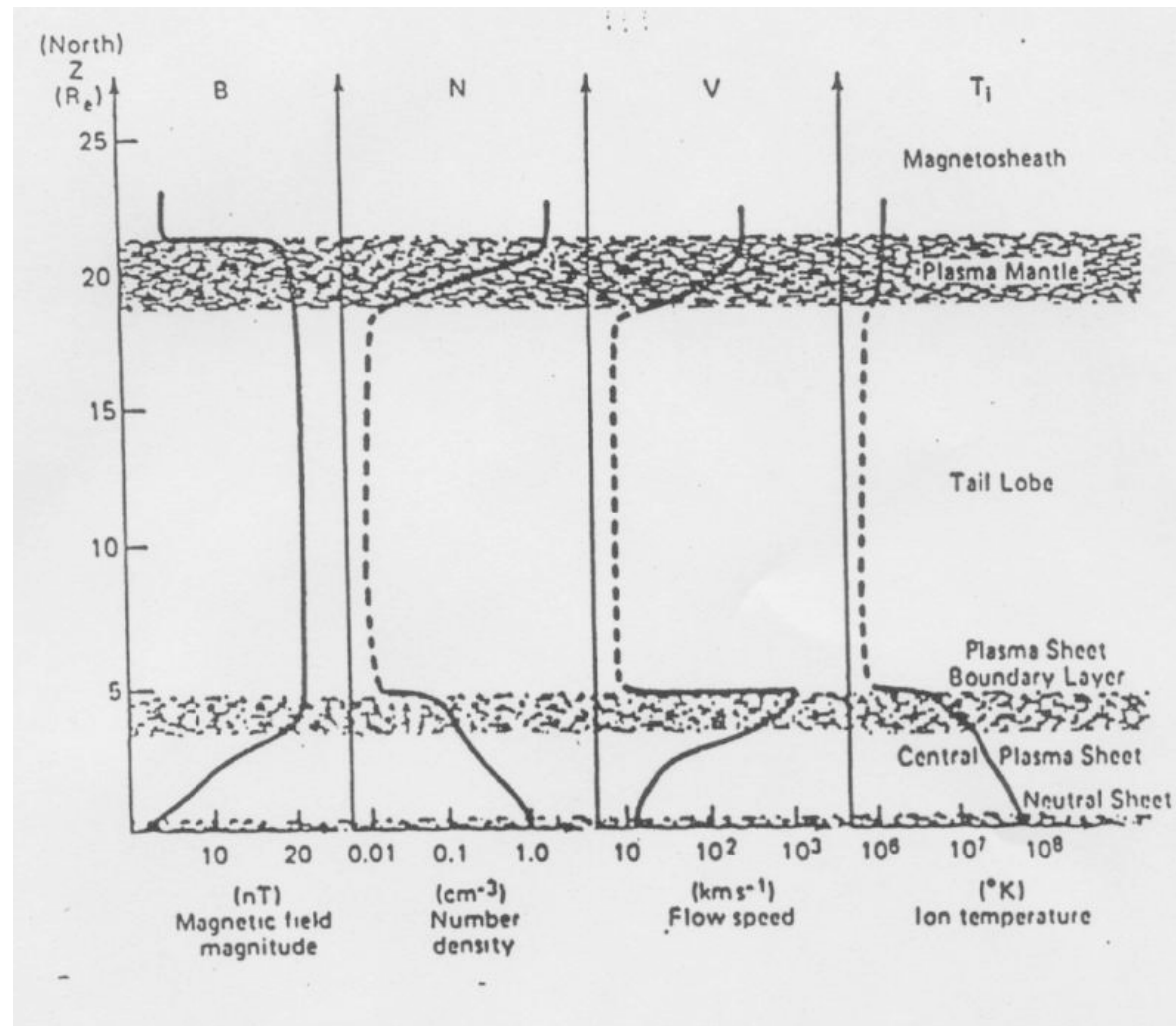
Laboratory observations

Space-lab interrelationship

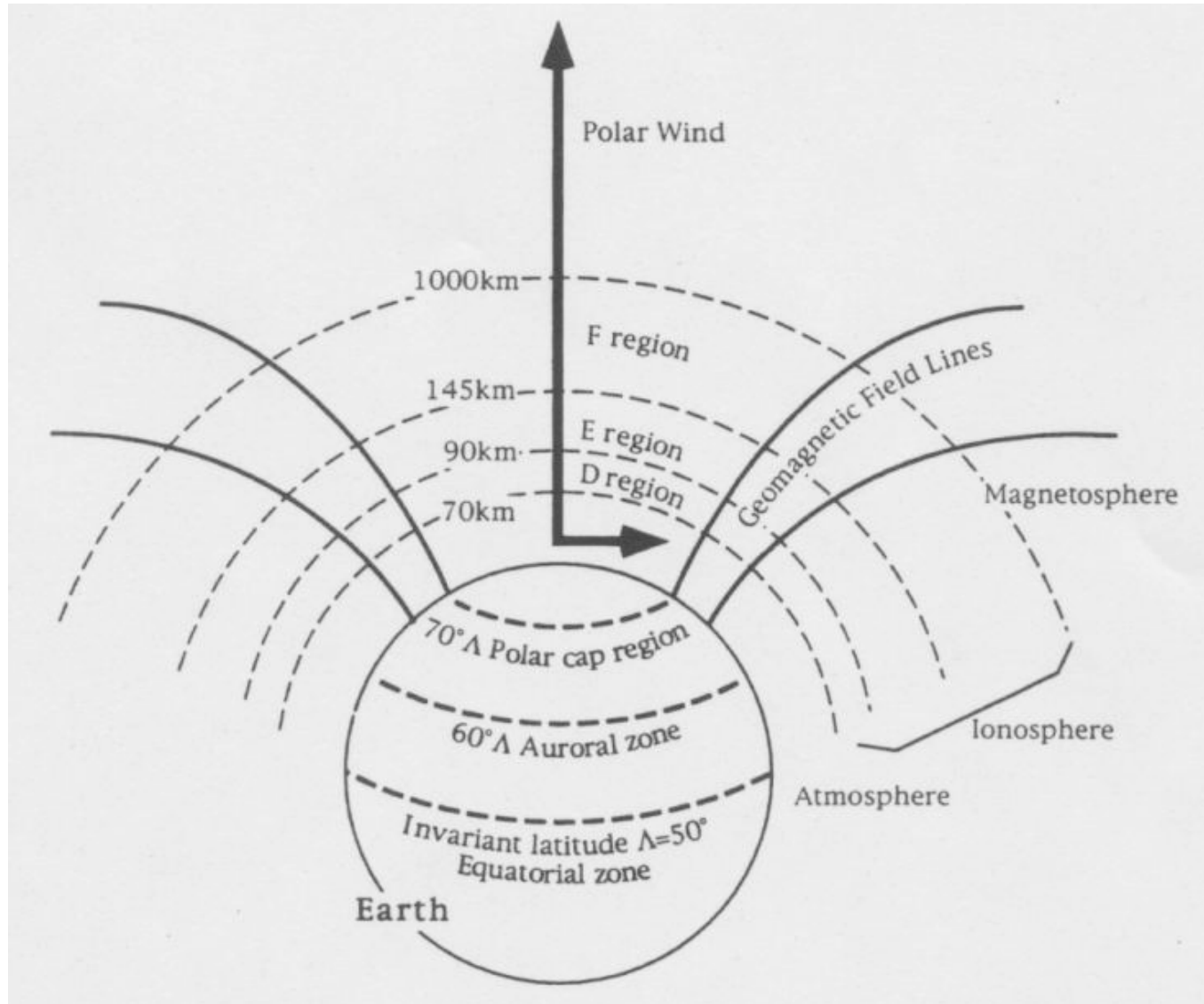
Earth's magnetosphere



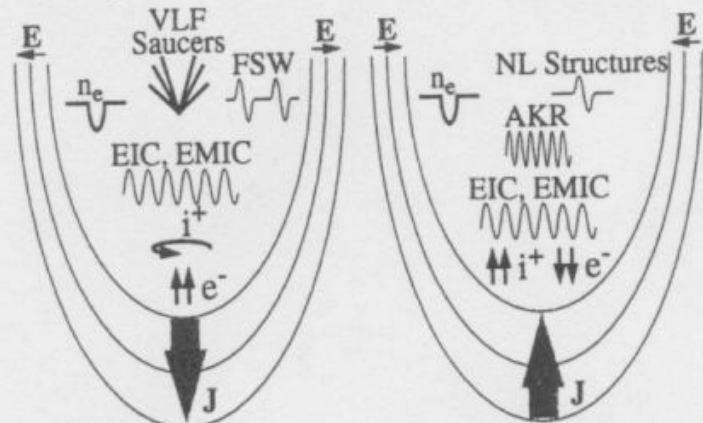
Spatial variation of ion beams at the plasma-sheet boundary layer



Regions of the ionosphere



The Symmetric Auroral Current Regions



- | | |
|--|--|
| 1. Downward current region.
$\downarrow\downarrow J$ | 1. Upward current region.
$\uparrow\uparrow J$ |
| 2. Diverging electrostatic shocks.
$E \ E$ | 2. Converging electrostatic shocks.
$E \ E$ |
| 3. Small-scale density cavities.
n_e
 | 3. Large-scale density cavity.
n_e
 |
| 4. Up-going, field-aligned electrons. Counter-streaming electrons.
$\uparrow\uparrow e^-$ | 4. Down-going, "inverted-V" and field-aligned electrons.
$\uparrow\uparrow e^-$ |
| 5. Ion heating transverse to B. Energetic ion conics.
 | 5. Up-going ion beam. Ion conics.
$\uparrow\uparrow i^+$ |
| 6. ELF electric field turbulence. Ion cyclotron waves.
 | 6. Large-amplitude ion cyclotron waves and electric field turbulence.
 |
| 7. Fast solitary waves: three-dimensional, rapidly moving electron holes.
 | 7. Nonlinear, time-domain structures associated with ion cyclotron waves.
 |
| 8. VLF saucer source region.
 | 8. AKR source region.
 |

Concept of shear implies orthogonal “flow” and “inhomogeneity” directions

- Fluid definition of shear allows for nonzero $n^{-1}d\langle nv_{dy,z}\rangle/dx$
- Kinetic definition of shear requires nonzero $dv_{dy,z}/dx$
- Concentrate on dv_{dy}/dx and dv_{dz}/dx , for
 - magnetic-field axis z (no z dependence)
 - inhomogeneity axis x , and
 - flow along either y axis or z axis.

Measurement of shear in space

- Perpendicular-flow shear
 - Measure the perpendicular electric field $E_{\perp}(t)$
 - Express rate of change in terms of ion flow E_{\perp}/B :
 $dE_{\perp}/dt = v_{dyi} dE_{\perp}/dx = (E_{\perp}/B)(dE_{\perp}/dx) = E_{\perp} dv_{dyi}/dx$
 - Rearranging, $dv_{dyi}/dx = E_{\perp}^{-1} dE_{\perp}/dt$
- Parallel-flow shear
 - Measure ion beam energy
 - Express beam energy in terms of beam velocity
 - Translate between time and space coordinates

Measurement of shear in the lab

- Perpendicular-flow shear
 - Measure ion perp-velocity distribution $f_{0i}(r, v_\theta)$
 - Determine radial profile of ion flow velocity $v_{d\theta i}(r)$
 - or use energy analyzer to infer $f_{0i}(r, v_\theta)$
 - or use emissive probe to infer $v_{d\theta i}(r)$ from $E_r(r)/B$
- Parallel-flow shear
 - Measure ion parallel-velocity distribution $f_{0i}(r, v_z)$
 - Determine radial profile of ion flow velocity $v_{dzi}(r)$
 - or use energy analyzer to infer $f_{0i}(r, v_z)$

Space values of perp-flow shear

- $0.1\text{s}^{-1} < (dv_{\text{dyi}}/dx) < 1\text{s}^{-1}$
 - Hilat satellite *Tsunoda et al. [1989]* 800 km
- $1\text{s}^{-1} < (dv_{\text{dyi}}/dx) < 5\text{s}^{-1}$
 - AE-D satellite *Basu et al. [1984]* 400 km
 - DE-2 satellite *Basu et al. [1988]* 400-900 km
 - FAST satellite *McFadden et al. [1998]* 4000 km
 - Freja satellite *Hamrin et al. [2001]* 1700 km
- $5\text{s}^{-1} < (dv_{\text{dyi}}/dx) < 25\text{s}^{-1}$
 - Javelin rocket *Kelley and Carlson [1977]* 400 km
 - DE-2 satellite *Basu et al. [1988]* 400-900 km
 - SCIFER rocket *Bonnell et al. [1996]* 400 km
 - AT2 rocket *Pietrowski et al. [1999]* 400 km
 - SCIFER rocket *Kinter et al. [2000a,2000b]* 400 km

Space values of parallel-flow shear

- $0.01\text{s}^{-1} < (dv_{\text{dzi}}/dx) < 0.1\text{s}^{-1}$
 - Hawkeye satellite *Kintner* [1976] 125000km
 - DE-2 satellite *Loranc et al.* [1991] 300 km
- $0.1\text{s}^{-1} < (dv_{\text{dzi}}/dx) < 5\text{s}^{-1}$
 - DE-2 satellite *Heelis et al.* [1984] 900km
 - DE-2 satellite *Basu et al.* [1988] 400-900 km
 - Freja satellite *Knudsen and Wahlund* [1998] 1400km
 - Cluster *Nykyri et al.* [2003] $8R_E$
 - Cluster *Nakamura et al.* [2004] $10R_E$
- $5\text{s}^{-1} < (dv_{\text{dzi}}/dx) < 500\text{s}^{-1}$
 - *McFadden et al.* [1998] *Gavrishchaka et al.* [2000]
 - *Koepke et al.* [2003] FAST satellite 4000km
- Other space observations
 - OGO 5 satellite *D'Angelo* [1973] $40R_E$
 - HEOS 2 satellite *D'Angelo et al.* [1974] $40R_E$
 - AE-C satellite *Potemra et al.* [1974] 600 km
 - EISCAT Radar *Oksavik et al.* [2004] 250 km

Lab values of perp-flow shear

- $0.1 < (dv_{dyi}/dx)/f_{ci} < 0.5$
 - Kent et al. [1969] Jassby [1972]
 - van Niekerk et al. [1991] Amatucci et al. [1994]
 - Koepke et al. [1994, 1995, 1998, 1999]
- $0.5 < (dv_{dyi}/dx)/f_{ci} < 1$
 - Yoshinuma et al. [1999, 2001] Carroll et al. [2003]
 - Kaneko and Hatakeyama [2005] Reynolds et al. [2005a]
- $1 < (dv_{dyi}/dx)/f_{ci} < 5$
 - Sato et al. [1986] Nielsen et al. [1992]
- $10 < (dv_{dyi}/dx)/f_{ci} < 100$
 - Yamada and Owens [1977] Mostovych et al. [1989]
 - Peyser et al. [1992] Thomas et al. [2005]
- $100 < (dv_{dyi}/dx)/f_{ci} < 1000$
 - Amatucci et al. [1996, 1998] Walker et al. [1997]
 - Matsubara and Tanikawa [2000] Amatucci et al. [2003]

Fusion applications of perp-flow shear

- *Wagner et al.* [1982] Tokamak
- *Erckman et al.* [1993] Stellarator
- *Sakai et al.* [1993] Mirror trap
- *Burrell* [1997] Tokamak
- *Tynan et al.* [2001] CSDX
- *Ellis et al.* [2001] MRX

Lab values of parallel-flow shear

- $0.1 < (dv_{\text{dzi}}/dx)/f_{\text{ci}} < 0.5$
 - *Wang et al. [1998]* *Agrimson et al. [2001,2002]*
 - *Koepke et al. [2002]* *Teodorescu et al. [2002a,b]*
 - *Kaneko et al. [2003]* *Reynolds et al. [2005b]*
- $0.5 < (dv_{\text{dzi}}/dx)/f_{\text{ci}} < 1$
 - *D'Angelo and von Goeler [1966]* *An et al. [1996]*
 - *Willig et al. [1997]* *Merlino et al. [1998]*

$$\sigma_{0i}^2 = 1 - (k_y/k_z)(dv_{\text{dzi}}/dx)/\omega_{ci}$$

$$\sigma_{ni}^2 = [1 - (k_y/k_z)(dv_{\text{dzi}}/dx)(1 - \{n\omega_{ci}/\omega\})/\omega_{ci}]$$

k_y/k_z differs for drift, acoustic, and cyclotron waves

Kelvin-Helmholtz instability depends on second derivative of perpendicular-flow velocity

- Energy associated with flow velocity $\propto v_y^2$

$$\langle v_y(x_0+x_1) \rangle = v_y(x_0) + v'_y(x_0)\langle x_1 \rangle + v''_y(x_0)\langle x_1^2 \rangle / 2$$

$$\langle v_y(x_0+x_1) \rangle^2 - \langle v_y(x_0) \rangle^2 = v_y(x_0)v''_y(x_0)\langle x_1^2 \rangle$$

Instability when $v_y v''_y < 0$

Shear effects

- Inhomogeneity results in discrete eigenmodes
Extra eigenmodes have different k_y, k_z values, allowing Landau resonance to optimize. $\varepsilon = \rho_i/L$

- Parallel-velocity shear shifts mode frequency

$\sigma_{0i}^2 = 1 - (k_y/k_z)(dv_{dzi}/dx)/\omega_{ci}$ is dv_{dzi}/dx dependent and frequency changes as shear increases. $\omega = \sigma k_z c_s$

Landau resonance changes as frequency shifts.

- Parallel-velocity shear destabilizes harmonics

$\sigma_{0i}^2 = 1 - (k_y/k_z)(dv_{dzi}/dx)/\omega_{ci}$ depends on k_y . Higher harmonics have larger m number. $\lambda = 2\pi r/m$; $k_y = m/r$

Primary characteristics of shear-driven waves can be categorized by freq. and $k_\theta \rho_i$

<u>Perp.-velocity shear</u>	ω_R	$k_\theta \rho_i$	dv_θ/dr
DRIFT	$\omega_e^* \pm k_\theta v_E$	0.15 – 0.3	$< \omega_e^*$
ION-CYCLOTRON	$\omega_{ci} \pm k_\theta v_E$	0.4 – 1.5	$< \omega_{ci}$
LOWER-HYBRID	$\omega_{LH} \pm k_\theta v_E$	1.8 – 4	$> \omega_{LH}$

<u>Parallel-velocity shear</u>	ω_R	$k_\theta \rho_i$
DRIFT	$\omega_e^*/2 + \sqrt{[(\omega_e^*/2)^2 + (\sigma_0 k_z c_s)^2]}$	0.3
ION-Acoustic	$\sqrt{[(\sigma_0 k_z c_s)^2]}$	0.5
ION-CYCLOTRON	$n\omega_{ci} + \sqrt[3]{[(\sigma_n k_z v_{thi})^2 n \omega_{ci} (T_e/T_i) \Gamma_n]}$	1 – 1.5
$\sigma_n^2 \equiv 1 - \frac{k_y}{k_z} \frac{dv_{diz}/dx}{\omega_{ci}} \left(1 - \frac{n\omega_{ci}}{\omega} \right)$		

Perpendicular-Velocity Shear was found to cause:

- decrease in excitation-threshold current
- increase in the azimuthal wave-number
- large shifting and broadening in frequency
- increase in the oscillation amplitude.

Measurements of the linear properties of the mode verified the predictions from Ganguli's model and motivated detailed investigations of the model to significantly extend the range, detail, and interpretation of its predictions.

Parallel-Velocity Shear (1)

- The consequence of a spatially varying parallel drift speed was investigated theoretically for cases of sharply [Chandrasekhar, 1961] and smoothly [D'Angelo, 1965] inhomogeneous velocity profiles.
- D'Angelo [1965] predicted a purely growing, electrostatic, ion instability driven by parallel-velocity shear. Lakhina [1987] and Gavriishchaka *et al.* [1998] predicted dissipative instabilities driven by parallel-velocity shear.
- We measure frequency in the lab frame ω_{lab} , whereas, in the drifting ion frame, the frequency ω_1 is equivalent to $\omega_{lab} - k_z v_{di}$. Using ω_1 , we can obtain the wave phase velocity $v_{\phi z}$ ($=\omega_1/k_z$) and compare $v_{\phi z}$ to velocities associated with positive and negative slope in the distribution function.
- Conceptually, introducing parallel-velocity shear causes a diamagnetic drift similar to that caused by a density gradient [Gavriishchaka *et al.*, 1998].
- Smith and von Goeler [1968] express the shear-induced, off-diagonal elements of the pressure tensor and show that they contain the factor k_y .

Parallel-Velocity Shear (2)

- Even for large parallel electron drifts $v_{de}/v_{ti} \gg 1$, ion-acoustic waves are strongly ion-Landau damped in homogeneous, isothermal plasma.
- For inhomogeneous plasma, the frequency depends on velocity shear.
- D'Angelo's instability corresponds to $\sigma^2 < 0$. Shear-modified ion-acoustic waves are associated with $\sigma^2 > 0$, having parallel wave-phase speed σc_s .
- For higher frequency, the $n > 0$ ion-cyclotron resonance, along with the $n = 0$ Landau resonance, must be included in evaluating the wave-particle interaction [Lakhina, 1987; Gavriishchaka et al., 2000].
- For ion-cyclotron waves, it is possible for the factor containing shear to become negative, in which case ion-cyclotron growth contributes to the overall growth of the ion-cyclotron waves.

Dispersion Relation with Sheared Ion Flow

Ion-acoustic waves ($u \equiv k_z/k_y$):

$$\sum_{n=-\infty}^{\infty} \left[\frac{\omega_1}{\sqrt{2k_z^2 v_{ti}^2}} Z \left\{ \frac{\omega_1 - n\omega_{ci}}{\sqrt{2k_z^2 v_{ti}^2}} \right\} + \frac{dv_{di}/dx}{2u\omega_{ci}} Z' \left\{ \frac{\omega_1 - n\omega_{ci}}{\sqrt{2k_z^2 v_{ti}^2}} \right\} \right] \Gamma_n(b_i) + \tau(1+F_{0e}) + 1 + k^2 \lambda_{Di}^2 = 0$$

$$\sigma_i^2 + \sigma_e^2 \frac{T_i}{T_e} + \sigma_i^2 \frac{\omega - k_z v_{di}}{\sqrt{2k_z^2 v_{ti}^2}} Z \left\{ \frac{\omega - k_z v_{di}}{\sqrt{2k_z^2 v_{ti}^2}} \right\} + \sigma_e^2 \frac{T_i}{T_e} \frac{\omega - k_z v_{de}}{\sqrt{2k_z^2 v_{te}^2}} Z \left\{ \frac{\omega - k_z v_{de}}{\sqrt{2k_z^2 v_{te}^2}} \right\} = 0$$

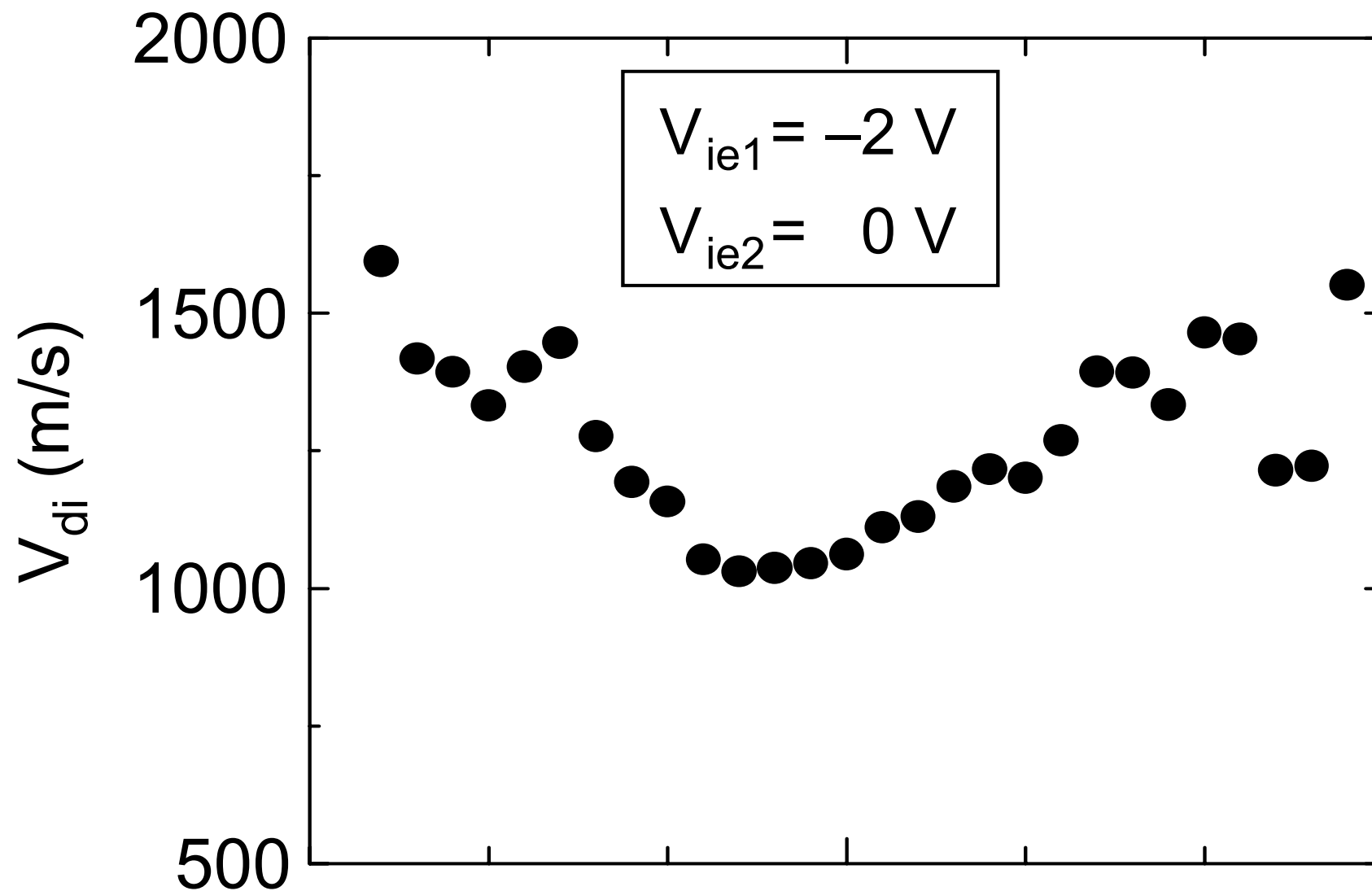
where $\sigma_i^2 \equiv 1 - (dv_{di}/dx)/(u\omega_{ci})$ and $\sigma_e^2 \equiv 1 + (dv_{de}/dx)/(u\omega_{ce})$.

Ion-cyclotron waves:

$$\sum_{n=-\infty}^{\infty} \Gamma_n(b_i) \left[\left(\zeta_0 + \frac{k_y dv_{di}/dx}{k_z \omega_{ci}} \right) \text{Im}Z\{\zeta_{ni}\} \right] + \tau \left(1 + \frac{k_y dv_{de}/dx}{k_z \omega_{ce}} \right) \text{Im}Z\{\zeta_{0e}\} = 0$$

$$\gamma/\omega_{ci} \propto \frac{\tau^{3/2}}{\mu^{1/2}} \left(\frac{k_z v_{de}}{\omega_{lr}} - 1 \right) - \sum_{n=-\infty}^{\infty} \Gamma_n(b_i) \left[1 - \frac{dv_{di}/dx}{u\omega_{ci}} \left(1 - \frac{n\omega_{ci}}{\omega_{lr}} \right) \right] \exp \left(-\frac{(\omega_{lr} - n\omega_{ci})^2}{2k_{||}^2 v_{ti}^2} \right)$$

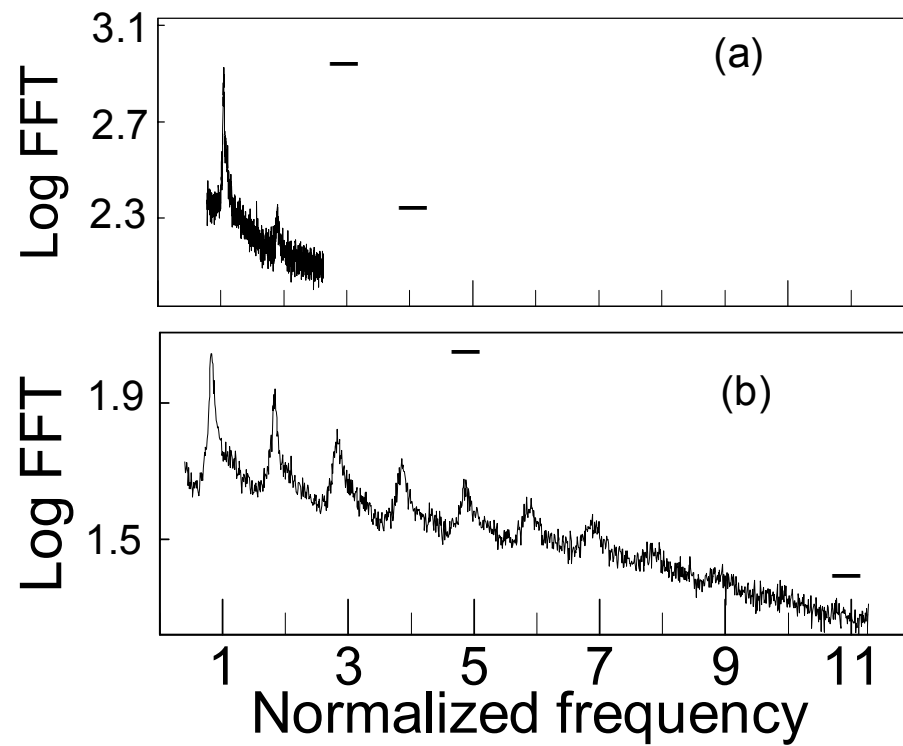
Radial Profile of Velocity Shear



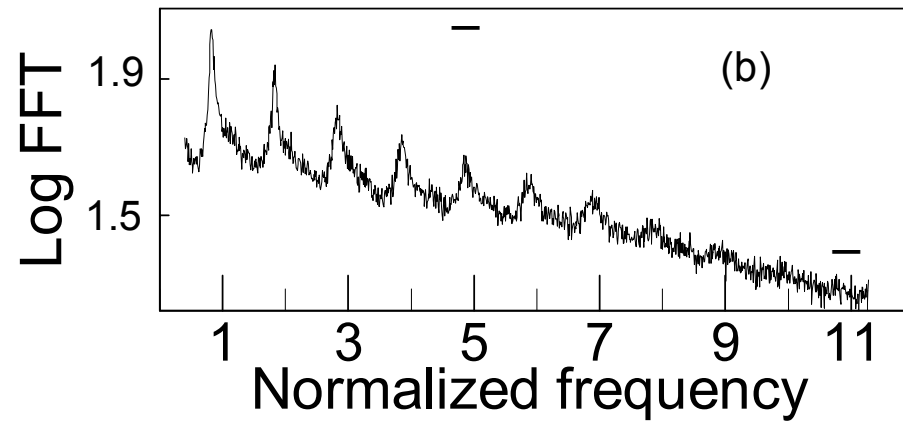
Harmonic Spectrum of SMIC in the laboratory

[Agrimson *et al.*, 2002; Teodorescu *et al.*, 2002]

No Shear



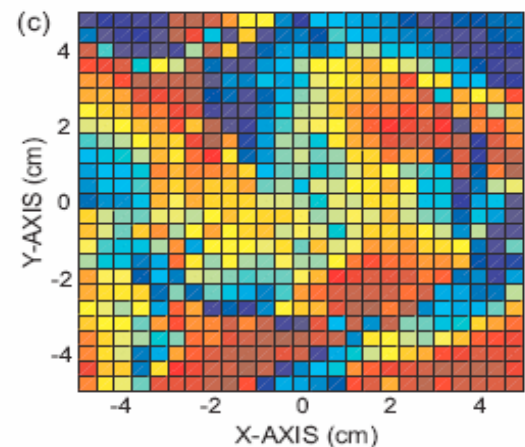
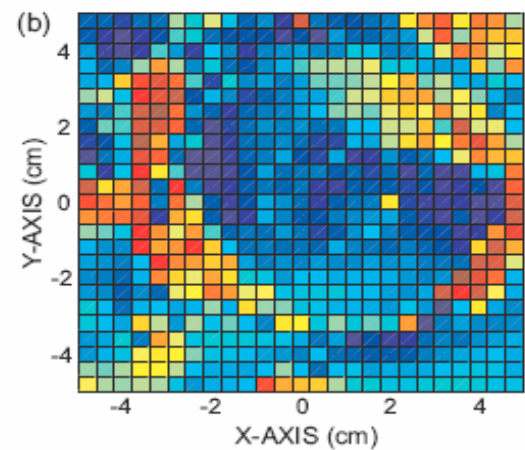
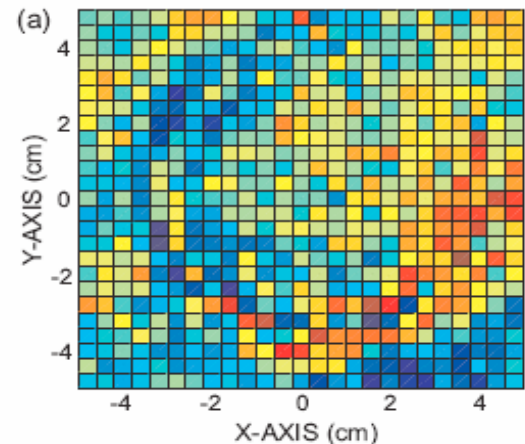
Shear



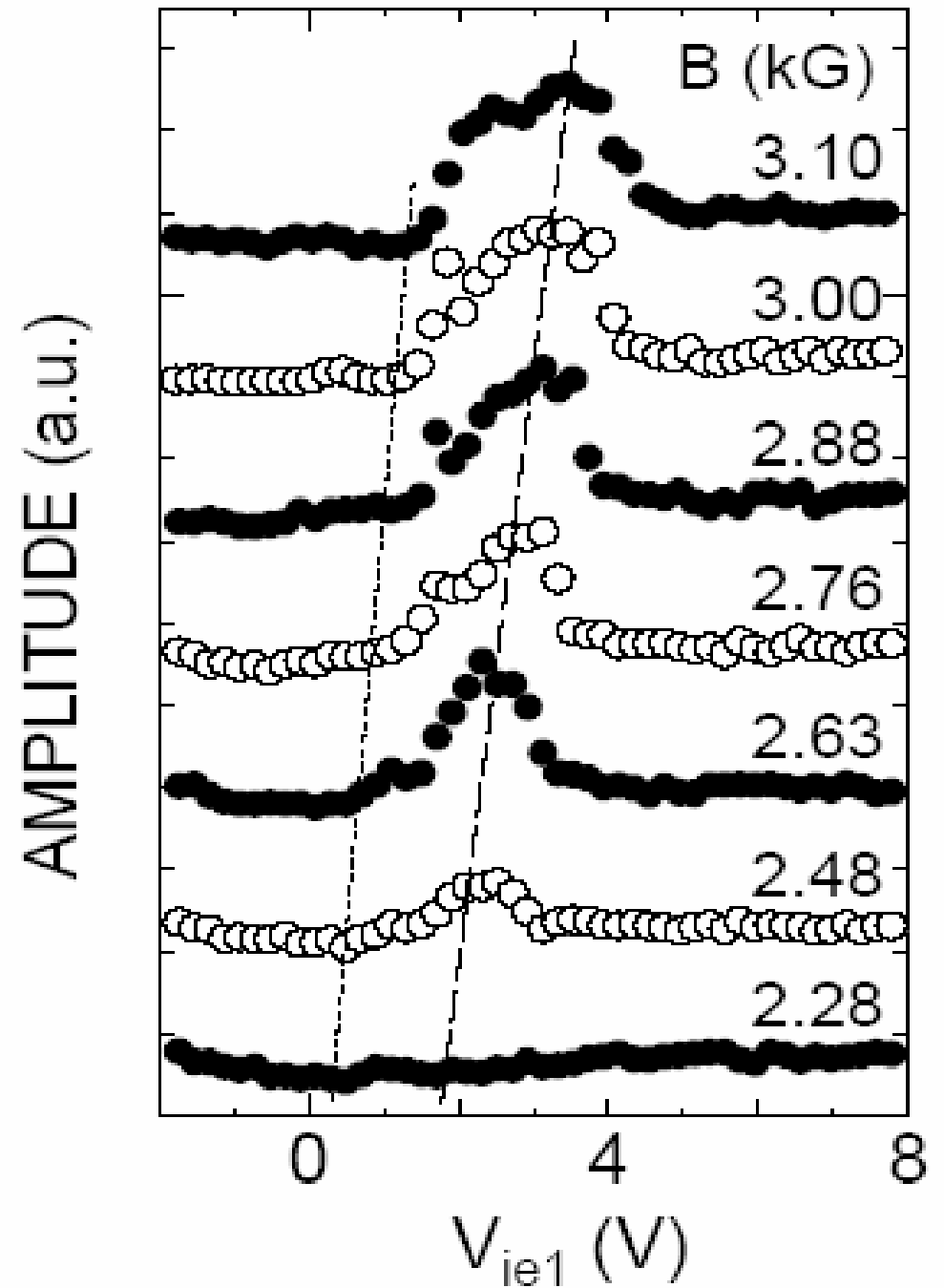
Lowest frequency mode corresponds to $m=1$ azimuthal mode.

Middle-frequency mode corresponds to $m=2$ azimuthal mode.

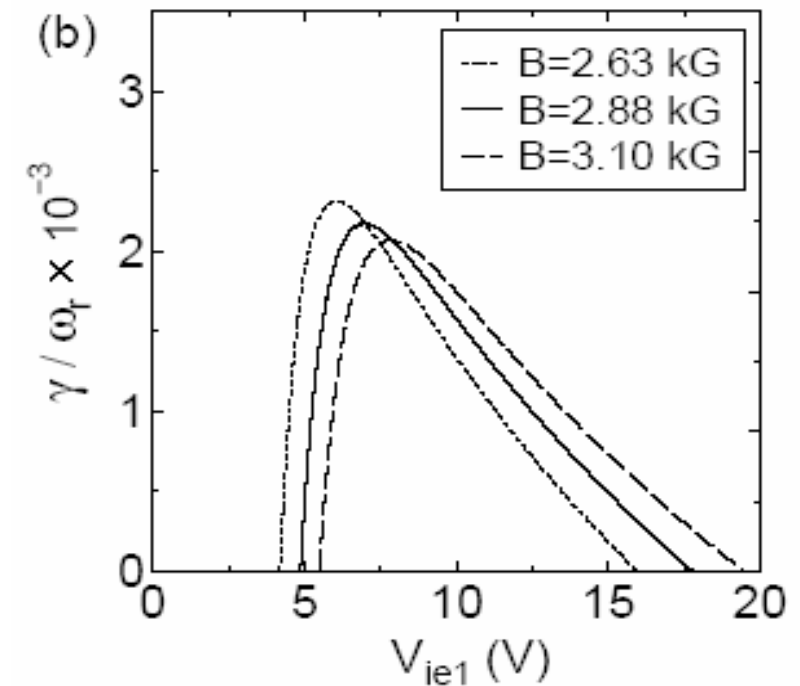
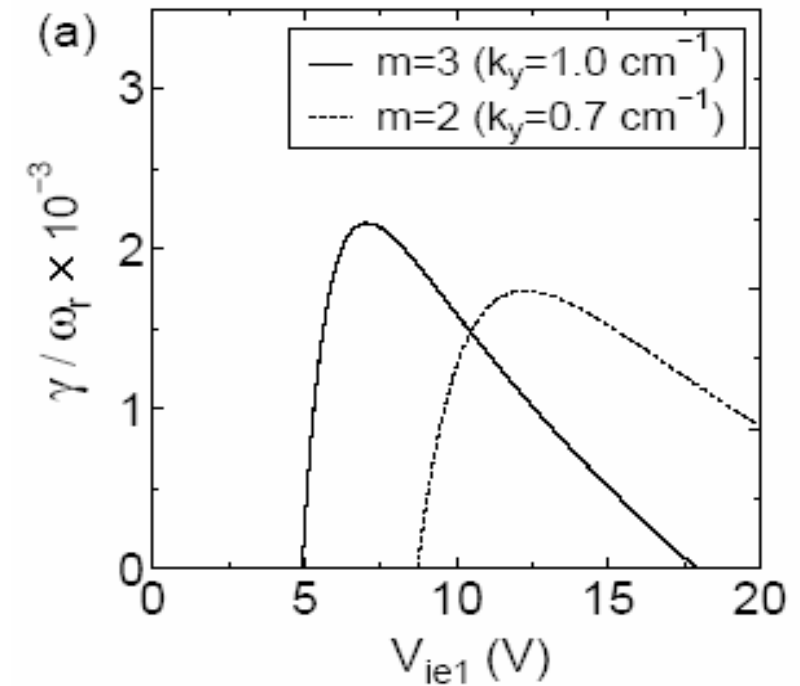
Highest frequency mode corresponds to $m=3$ azimuthal mode.



Excitation shear-threshold (dashed line) for a specific mode depends on magnetic field, as expected from σ . Ignore bottom two lines.



Experimental results
agree qualitatively
with analytical
theory predictions.



Conclusions

- Diagnostics sufficient for measuring shear
- Wide range of shear values in space/lab
- Width of shear profile also important
- Five effects of shear
 - KH mechanism from energy principle: $v_y v''_y < 0$
 - IEDD-reactive mechanism is like two-stream: $\omega(\omega - k_y v_y)$
 - IEDD-dissipative mechanism alters dispersion: $\varepsilon = \rho_i/L$
 - Shear modification shifts mode frequency: $\omega = \sigma k_z c_s$
 - Shear modification destabilizes harmonics: $\lambda = 2\pi r/m$; $k_y = m/r$
- Observational signatures indicate these effects
- Role of σ is experimentally verified via thresholds

$$\sigma_{ni}^2 = [1 - (k_y/k_z)(dv_{dzi}/dx)(1 - \{n\omega_{ci}/\omega\})/\omega_{ci}]$$